J. Am. Chem. Soc. **1995,** *117,* 6497–6503

Gas-Phase Reactions of Catecholate and Related Anions with BF_3 and SiF_4

W. S. Taylor[†] **and Lucia M. Babcock***,[‡]

Contribution from the Department of Chemistry, Louisiana State University, Baton Rouge, Louisiana 70803

Received June 24, 1993[®]

Abstract: The gas-phase reactions of the anions of catechol, 4-methylcatechol, resorcinol, and *o*-cresol with BF_3 and SiF_4 have been examined using the flowing afterglow technique. These systems initially form an addition product in a three-body step, and this addition product subsequently participates in fluoride transfer with a second molecule of the reactant neutral. The reactions involving the anions of catechol and 4-methylcatechol exhibit a second primary product channel which is independent of the concentration of the third-body. Results suggest that this bimolecular product is a cyclic species formed in a step involving the ring-closure step and loss of HF. Relative amounts of the two primary products are sensitive to pressure as well as to the identity of the Lewis acid. We explain this behavior in terms of a multiple-well potential energy surface which contains a barrier in the bimolecular product channel.

Introduction

We have been interested in the ion–molecule (IM) reactions of several phenolic anions with Lewis acids in the gas phase. Specifically, we have examined the reactions of the negative ions of catechol (1,2-dihydroxybenzene), 4-methylcatechol (1,2-dihydroxy-4-methylbenzene), resorcinol (1,3-dihydroxybenzene), and *o*-cresol (1-hydroxy-2-methylbenzene) with BF_3 and SiF_4 using the flowing afterglow technique. Catechol and the substituted catechols are an extremely versatile and important class of molecule. They are frequently physiologically active (L-dopa, l-epinephrine, and norepinephrine are substituted catecholamines) and their reactivities with transition metals in solution are well-known.[1–4] These compounds have received attention from the standpoint of biologically related studies, but the simple catechols are attractive for study in less complicated systems as well, having several features which make them interesting ligands. First, their structure is unique among dihydroxy compounds. The aromatic ring keeps the ligand rigid and defines the relative orientation of the two hydroxyl groups; this lack of flexibility has been shown to be important in the solution reactions of catechol and substituted catechols with trigonal boron acids.[5] Second, the acidity range of the substituted catechols is quite broad, allowing an examination of the effects of ligand acidity upon reactivity without altering the unique structural character of the ligand. Third is perhaps the most interesting feature of the catechols—they can be either monodentate or bidentate. In conjunction with the rigid structure of these diols, this is especially interesting since coordination of the first hydroxy group orients the second for subsequent ring closure. We have carried out what to our knowledge are the first gas-phase mechanistic studies of these ligands in our examination of reactions of BF_3 and SiF_4. The solution reactions of catechol and substituted catechols with trigonal boron acids have been studied extensively, and kinetic studies show that coordination of the first hydroxyl group to the central boron atom is rate determining and that it is followed by rapid ring closure.[5–7] The only complexes which have been observed in solution are those in which both oxygens are bonded to the boron atom to form the tetrahedral anion in which catechol is bidentate; the monodentate complex has never been observed. Similarly, there have been extensive studies of reactions of tetracoordinate Si species with several aliphatic and aromatic diols as well as with 2-hydroxy carboxylic acids in solution. These have demonstrated that cyclic bidentate anions involving pentacoordinate Si anions are formed easily in solution.[8] But here also there are no examples of formation of the monodentate anion. Results from the reactions we have studied in the gas phase differ markedly from the solution results in that both monodentate and bidentate products are observed; in fact, production of the monodentate anion is the favored reaction channel. Examination of these systems in the absence of complicating solvent effects allows us to elucidate intrinsic details concerning complexation, and knowledge of the specific reactive nature of these systems in the gas phase allows us to make inferences regarding the potential energy surfaces upon which these reactions occur. While the formation of these particular products is expected on the basis of solution analogues, the distribution of products is not. Indeed the observation of an intermediate which is not observed in solution reactions affords the opportunity to examine details of internal nucleophilic attack and subsequent ring closure.

All four of the anions examined here can add to the Lewis acids via a three-body process resulting in a four-coordinate boron anion or in a five-coordinate silicon anion in which the ligand is monodentate. For catechol and 4-methylcatechol, the second –OH group can then react in a ring-closure step to form a bidentate anionic species with concomitant loss of HF. As mentioned above, in analogous solution reactions only the ring-closed anion is observed for reactions of trigonal boron acids with diols;[5–7] in the gas phase, however, both monodentate and bidentate products are observed for reactions of BF_3 and SiF_4 with the 1,2-dihydroxy anions. Reactions of the anions of

---

[†] Current address: Department of Chemistry, University of Central Arkansas, Conway, AR 73032.

[‡] Current address: Department of Chemistry, University of Georgia, Athens, GA 30602.

[®] Abstract published in *Advance ACS Abstracts,* February 1, 1995.

(1) Gilbert, K.; Kustin, K. *J. Am. Chem. Soc.* **1976**, *98*, 5502.

(2) Jones, S. E.; Chin, D.-H.; Sawyer, D. T. *Inorg. Chem.* **1981**, *20*, 4257.

(3) Bosserman, P. J.; Sawyer, D. T. *Inorg. Chem.* **1982**, *21*, 1545.

(4) Bodini, M. E.; Copia, G.; Robinson, R.; Sawyer, D. T. *Inorg. Chem.* **1983**, *22*, 126.

(5) Pizer, R.; Babcock, L. M. *Inorg. Chem.* **1977**, *16*, 1677.

(6) Babcock, L. M.; Pizer, R. *Inorg. Chem.* **1980**, *19*, 56.

(7) Babcock, L. M.; Pizer, R. *Inorg. Chem.* **1983**, *22*, 174.

(8) Corriu, R. J. P.; Young, J. C. In *The Silicon–Heteroatom Bond*; Patai, S., Rappoport, Z., Eds.; John Wiley & Sons Ltd.: New York, 1989.

0002-7863/95/1517-6497$09.00/0

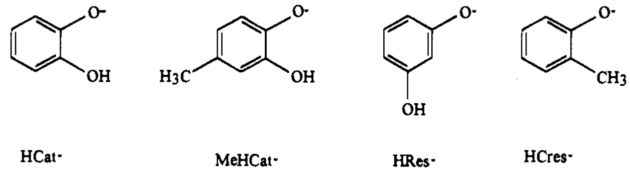

Figure 1. Structures and abbreviations for ligand anions of catechol, 3-methylcatechol, resorcinol, and *o*-cresol are given.

resorcinol and *o*-cresol were carried out in an effort to elucidate specific mechanistic details regarding ring-closure in the other two systems. While the reactions of the anions of resorcinol and *o*-cresol with both Lewis acids can yield monodentate addition products, these ions cannot participate in a ring-closure step. The structures of all the reactant ions examined in this work are given in Figure 1. By examining factors affecting the competition between the two product channels we gain information about the barriers present in these channels, and by comparison to solution results, we obtain insights into solvent modification of these reactions.

Experimental Section

The majority of reactions examined here were carried out on a flowing afterglow reactor which has been described previously.[9] In general, the flowing afterglow is a fast-flow gas-phase reactor which operates in the laminar flow regime. In a typical flowing afterglow experiment, an inert carrier gas (usually He) is introduced into the upstream end of the flow tube. Production of the reactant ion is often carried out via electron impact on a source gas, but a variety of other ionization methods can also be employed. Negative reactant ions are produced via electron attachment, electron transfer, or chemical ionization. After production of the reactant ions, the gas mixture flows into a thermalization zone. Neutral reactants are injected at one of two ports located at different axial positions along the flow tube in order to provide two reaction distances. The reaction then proceeds for the amount of time required for the reaction mixture to flow through the reaction zone. Sampling of the reaction mixture is carried out via a 0.3 mm orifice. Reactant and product ions are then analyzed with the use of a quadrupole mass filter. Mass-selected ions are detected with an electron multiplier. Rate information is obtained by monitoring the decay of reactant ion and the growth of product ions as a function of neutral reactant gas flow. Reported rate coefficients are averages of several kinetic runs and are reproducible to within ±10%.

Catechol (H_2Cat) and resorcinol (H_2Res), both with purities of approximately 99%, were obtained from Sigma. These compounds were further purified by vacuum sublimation before use in the reactions outlined here. The 4-methylcatechol (MeH_2Cat) was obtained from Aldrich with a purity of 99% and was used without further purification. This was also the case with *o*-cresol (H_2Cres), which was obtained from Aldrich with a purity of 99+%.

Catechol, resorcinol, and 4-methylcatechol are solids at room temperature and were introduced into the flow tube by placing them in small reagent bulbs which were then gently heated to temperatures ranging from 70 °C for catechol and 4-methylcatechol to 100 °C for resorcinol in order to enhance the sublimation rate of the solids. The vapor pressure of *o*-cresol at room temperature is sufficiently high that it did not require heating for adequate reactant ion production. All reagent bulbs were connected to the upstream end of the flow tube and were equipped with a flush line through which a small amount of the carrier gas was passed. Metering valves were placed on these flush lines as well as on the reagent bulbs themselves. By manipulating these flows, the amount of neutral precursor vapor admitted into the flow tube was adjusted for optimum reactant ion signal.

All of the reactant ions used in this study were generated via negative chemical ionization. This was carried out using two separate methods. The first method uses N_2O and CH_4 to form OH^- which then abstracts a proton from the neutral precursor of the desired ligand anion.[10] The second method uses NH_3 and H_2O to produce either NH_2^- or OH^- which then abstracts a proton from the neutral precursor. Anions of both 4-methylcatechol ($MeHCat^-$) and resorcinol ($HRes^-$) were generated via proton abstraction using the second method. Negative ions of *o*-cresol ($HCres^-$) were formed from the method using N_2O and CH_4 described above. Production of the catecholate anion ($HCat^-$) was accomplished using both of the chemical ionization techniques. Regardless of the method of ion production, the outcomes of the reactions examined here were independent of the method of ion production. Anhydrous ammonia, nitrous oxide, and methane were obtained commercially and used without further purification, as were the reactant neutrals BF_3 and SiF_4.

Table 1. Product Formation

reaction	primary products	secondary products	tertiary products
$BF_3 + HCat^-$	BF_3HCat^-	BF_4^-	$BF_3{\cdot}BF_4^-$
		$BF_3HCat^-{\cdot}BF_3$[a]	
	$BF_2Cat^- + HF$	$BF_2Cat^-{\cdot}BF_3$[a]	
$SiF_4 + HCat^-$	SiF_4HCat^-	SiF_5^-	
	$SiF_3Cat^- + HF$		
$BF_3 + MeHCat^-$	$BF_3MeHCat^-$	BF_4^-	$BF_3{\cdot}BF_4^-$
	$BF_2MeCat^- + HF$		
$SiF_4 + MeHCat^-$	$SiF_4MeHCat^-$	SiF_5-	
	$SiF_3MeCat^- + HF$		
$BF_3 + HRes^-$	BF_3HRes^-	BF_4^-	
$SiF_4 + HRes^-$	SiF_4HRes^-	SiF_5^-	
$BF_3 + HCres^-$	BF_3HCres^-	BF_4^-	$BF_3{\cdot}BF_4^-$

[a] Product observed in N_2 only.

Reactions were carried out in both helium and nitrogen carrier gases. Helium, with a purity of 99.995%, was further purified before introduction into the flow tube by passing it through molecular sieves immersed in liquid nitrogen. Ultra-high-purity nitrogen used as a carrier was likewise directed through molecular sieves cooled in a dry ice/acetone bath.

Results and Discussion

Product Formation. Reactions of $HCat^-$, $MeHCat^-$, and $HRes^-$ were carried out with both Lewis acids whereas experiments involving $HCres^-$ were performed with BF_3 only. These reactions are summarized in Table 1. Two general categories are apparent depending on the primary product(s) formed, i.e., those systems which form bimolecular products in addition to three-body products and those systems which yield only a three-body product. Reactions of BF_3 and SiF_4 with both $HCat^-$ and $MeHCat^-$ form bimolecular as well as three-body products, while $HRes^-$ and $HCres^-$ yield only three-body products. In all cases, the three-body product participates in a subsequent fluoride transfer step. As seen in Table 1, secondary and tertiary clustering steps are also observed for some reactions, although clustering involving primary products is seen only in the presence of N_2, which is a more efficient collisional stabilizer.[11] The reactions of $HCat^-$ and $MeHCat^-$ with BF_3 and SiF_4 involve a competition between the bimolecular channel and the three-body channel. This competition manifests itself in a branching ratio between the two which is dependent upon pressure (concentration of the third-body). Branching ratios for the three-body and bimolecular product ions were determined using a standard method in which the percentage of the total product ion signal represented by each product is plotted as a function of the extent of reaction (neutral flow).[12] When subjected to this analysis, our results clearly show that both of these ions are formed in primary steps. Primary product branching ratios were obtained in this way at several different

---

[9] Babcock, L. M.; Taylor, W. S.; Herd, C. R. *Int. J. Mass Spectrom. Ion Processes* **1987**, *81*, 259.

[10] DePuy, C. H.; Damrauer, R.; Bowie, J. H.; Sheldon, J. C. *Acc. Chem. Res.* **1987**, *20*, 127.

[11] Anicich, V. G.; Bowers, M. T. *J. Am. Chem. Soc.* **1974**, *96*, 1279.

[12] Adams, N. G.; Smith, D. *J. Phys. B: Atom. Mol. Phys.* **1976**, *9*, 1439.

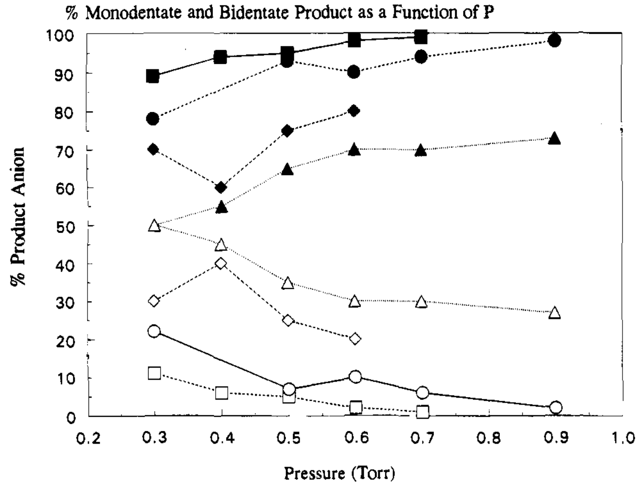

Figure 2. Product distributions as a function of pressure for the reactions of BF_3 + $MeHCat^-$ (squares), BF_3 + $HCat^-$ (circles), SiF_4 + $MeHCat^-$ (diamonds), and SiF_4 + $HCat^-$ (triangles) are presented. The solid symbols represent percentages of monodentate product while the open symbols represent percentages of bidentate product.

pressures, and the variation in primary product channel branching ratios as a function of pressure is shown in Figure 2. Reactions of $HCat^-$ with BF_3 and with SiF_4 were carried out in N_2 buffer gas, and product branching ratios showed the same behavior. Duplicate determinations at the same pressure were averaged and are generally reproducible to within ±5%.

The results of these reactions suggest the generalized reaction scheme given in eq 1 below:

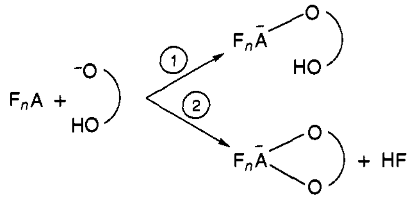

(1)

where F_nA represents the neutral Lewis acid (either BF_3 or SiF_4) and the bifunctional ligand anion is shown as a negatively charged oxygen donor ion and a protonated oxygen donor atom joined by some chain. Two primary product channels are shown, but as has been noted, access to both is observed for only two ligand anions. The three-body product corresponds to a monodentate species and the bimolecular product is a bidentate cyclic structure formed via loss of HF. These product structures are consistent with the condensed phase behavior of the catecholate anion as well as the behavior observed here for $HRes^-$ and $HCres^-$. As is shown in Table 1, no bimolecular products result from the reaction of these anions with either Lewis acid. The *meta* configuration of the −OH groups in $HRes^-$ precludes ring-closure to form the bidentate structure. Thus, the geometry of the two functional groups on the ligand ion is a determining factor in the formation of the bimolecular product. The $HCres^-$ results indicate that, in addition to an *ortho* configuration, the second functional group must be capable of itself donating a proton. Taken together, the behavior of these two ligand anions supports the assertion that the bimolecular product is cyclic, or that the reacting system passes through a cyclic transition state in order to access this product channel. In view of related solution studies,[5-8] these cyclic products are not surprising, but it is important to establish that they are formed in gas-phase reactions as well. What is unique about these studies in the gas phase is the opportunity to examine formation of the monodentate species (not observed in solution) and its subsequent elimination of HF to yield bidentate product anions.

Table 2. Average Rate Constants in He

anion	Lewis acid	pressure (Torr)	k_{obs}[a]	k_L[a]	k_{obs}/k_L
$HCat^-$	BF_3	0.25−0.70	4.9 ± 0.6	6.6	0.74
$HCat^-$	SiF_4	0.25−1.00	5.7 ± 0.5	7.5	0.76
$MeHCat^-$	BF_3	0.30−0.70	4.4 ± 0.8[b]	6.4	0.69
$MeHCat^-$	SiF_4[c]				
$HRes^-$	BF_3	0.31−0.60	4.6 ± 0.7	6.6	0.70
$HRes^-$	SiF_4	0.30−0.60	5.9 ± 0. 9	7.5	0.79
$HCres^-$	BF_3	0.30−1.00	5.2 ± 0.6	6.6	0.79

[a] All rate constants reported in units of 10^{-10} $cm^3 \cdot molecule^{-1} \cdot s^{-1}$. [b] Upper limit. [c] Rate data not obtained.

Kinetic Behavior. With regard to primary product formation, the sequence of reactions outlined above is consistent with the generalized mechanism given below:

$$\begin{tikzcd}
A^- + B \arrow[r, shift left, "k_a"] & (AB^-)^* \arrow[l, shift left, "k_d"] \arrow[r, "k_{bi}"] \arrow[d, "\beta k_s[M]"] & C^- + D \\
& AB^- &
\end{tikzcd} \qquad (2)$$

In this scheme, k_a, k_d, and k_{bi} are the microscopic rate constants for the association of the ion and the neutral, dissociation back to reactants, and bimolecular product formation, respectively; k_s is the three-body rate constant for formation of the association product, [M] is the concentration of the third-body, and β is the collision efficiency. The expression for the overall observed rate constant for this mechanism can be obtained by making the steady-state assumption for $(AB^-)^*$. The resulting expression is given in eq 3.

$$k_{obs} = \frac{k_a(\beta k_s[M] + k_{bi})}{k_d + \beta k_s[M] + k_{bi}} \qquad (3)$$

This general type of equation in which k_{obs} is a function of several microscopic rate coefficients has been successful in explaining temperature and pressure effects observed for both bimolecular and three-body IM processes. Studies of this nature have been reviewed extensively by Meot-ner.[13] Here, values for k_{obs} were measured in He over the pressure range 0.25−1.00 Torr. Under these conditions, the observed rate constants exhibit an apparent insensitivity to pressure. The exception to this generalization is the reaction of BF_3 + $MeHCat^-$, which exhibited a slight negative dependence on pressure. This negative pressure dependence is an artefact of experimental conditions as is discussed below. The results are summarized in Table 2 where the average rate constant for each process is reported for the given pressure range. In addition, the Langevin rate constant for each reaction is given, along with the fraction of the Langevin rate represented by the rate constants measured in this work. All of the values for k_{obs} reported here are 70−80% of the Langevin rate. The fact that these rate constants display no significant dependence on pressure suggests that the reactions are nearing saturation and the pressure dependence is negligible over the limited range of experimental pressures studied, or that they are in fact saturated with k values less than the upper limit calculated using Langevin theory. The reactions of $HCat^-$ with BF_3 and SiF_4 were also carried out using nitrogen as a buffer gas. Values for k_{obs} under these conditions are given in Table 3. The rate constants in nitrogen are higher at almost 90% of the Langevin collision rate constant, again illustrating the greater capability of N_2 to act as a collisional stabilizer.[11] The fact that the rate coefficient values are larger in nitrogen buffer gas than in helium buffer gas also indicates that the reactions are not saturated in He.

---

(13) Meot-ner, M. In *Gas Phase Ion Chemistry*; Bowers, M. T., Ed.; Academic Press: New York, 1979; Vol. 1.

Table 3. Average Rate Constants in N_2

anion	Lewis acid	pressure (Torr)	k_{obs}[a]	k_L[a]	k_{obs}/k_L
$HCat^-$	BF_3	0.13–0.40	5.9 ± 0.6	6.6	0.89
$HCat^-$	SiF_4	0.13–0.30	6.6 ± 0.8	7.5	0.88

[a] All rate constants reported in units of 10^{-10} $cm^3 \cdot molecule^{-1} \cdot s^{-1}$.

As has been noted, the observed rate constant for the reaction of BF_3 with $MeHCat^-$ displays a slight negative dependence on pressure. This is likely due to the presence of OH^- in the reaction zone of the flowing afterglow remaining from the production of $MeHCat^-$ from its neutral precursor. The presence of hydroxide ions can complicate kinetic measurements considerably, since reactant ions are being formed from the reaction of OH^- ions with the source neutral simultaneously with their depletion by reaction with BF_3 or SiF_4. Our observation of OH^- in the flow tube indicates that this species is present in the reaction zone of the FA. It has been shown, however, that OH^- is itself depleted by both BF_3 and SiF_4. The rate constants for reactions 4 and 5 have been determined using a SIFT reactor over a pressure range of 0.4–1.0 Torr and a temperature range of 205–450 K:[14]

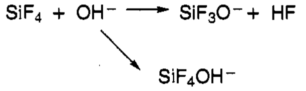
(4)

$$SiF_4 + OH^- \longrightarrow SiF_3O^- + HF \quad ; \quad SiF_4 + OH^- \longrightarrow SiF_4OH^-$$

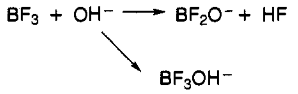
(5)

$$BF_3 + OH^- \longrightarrow BF_2O^- + HF \quad ; \quad BF_3 + OH^- \longrightarrow BF_3OH^-$$

Any hydroxide ions present in the reaction zone will be consumed by one of these processes. Thus, a competition for the OH^- ions exists between the Lewis acid and the source neutral for the desired bifunctional reactant ion. In addition, the reactant ion continues to be depleted by the Lewis acid. Numerical modeling of this set of reactions has been carried out over a variety of simulated experimental conditions in order to determine the effect of OH^- on the reactions studied here. For all situations examined, the apparent rate of depletion of the reactant ion by the Lewis acid was shown to increase in the presence of OH^-, since the Lewis acid consumes not only the reactant ion but also a precursor of the reactant ion. The magnitude of this rate increase depends on the relative concentrations of all the reacting ions and upon the rate of proton abstraction from the source neutral, but the result is an apparent negative dependence of k_{obs} on pressure when OH^- is present in the reaction zone. These models demonstrate that if the ratio of OH^- to the bifunctional reactant ion is kept as small as possible, the effect of the presence of OH^- on the observed rate constant will be minimized.

In the systems examined here, hydroxide ions react faster with the reactant neutral than do the bifunctional reactant ions; thus, it was possible in most cases to make rate determinations after the OH^- was depleted. If this is not possible, as was true in the reaction of BF_3 with $MeHCat^-$, the observed rate constant must be treated as an upper limit. Rate determinations for the reaction of $MeHCat^-$ with SiF_4 were not carried out since the mass of one of the products in this process is the same as that of the reactant ion. Although rate information could not be obtained, product branching ratios as shown in Figure 2 could be obtained. The coincidental masses were the reactant ion, $MeHCat^-$, and the secondary product ion SiF_5^-. Branching ratios of the two primary products were obtained from extrapolation of data early in the reaction where the secondary product ion had not formed to an appreciable degree.

Competing Products and Potential Energy Surfaces. Since the observed rate constants for the reactions of $HRes^-$ and $HCres^-$ are comparable to those for the other two anions, we can conclude that the association reaction for all the anions is not significantly dependent upon either the nature or the relative geometry of the second functional group. This points to a mechanism which is dominated by formation of the association product (monodentate product) and suggests the presence of a barrier in the bimolecular product channel which lowers the efficiency for the formation of the bidentate product. The height of the barrier dictates the relative amounts of monodentate and bidentate ion products formed at a given pressure. If the barrier in the bimolecular product channel is very high, then no bimolecular products will be formed and only the monodentate species will be observed. For barriers of intermediate height, both products should be observed. Under these circumstances, we would expect the branching ratio to be dependent upon pressure and temperature, and be indicative (at least qualitatively) of the height of the barrier. If a very small potential barrier exists, then only the bimolecular products will be observed, assuming that their formation is energetically favorable. This behavior is analogous to what is observed in solution.[5–8] The reactions of $HCat^-$ and $MeHCat^-$ in the gas phase fall into the second category. The height of the barrier relative to reactants and products is determined by factors involved in the ring closure and HF elimination step. Such factors include ligand geometry and flexibility, coordination number of the central atom, ring size, and ligand donor atom identity. The methyl substituent on the aromatic ring in $MeHCat^-$ does not have a significant effect on product branching ratios in the reactions studied here. Rather, the barrier height appears to be largely dictated by constraints imposed on the ring closure step by the rigid geometry of the catecholate and substituted catecholate ligands. Solution studies of bidentate ligand anion coordination offer limited insights into details of the ring closure and elimination step because it proceeds so rapidly. The gas-phase studies provide information about this part of the potential energy surface as well as about intrinsic reactivities in the absence of solvent. Since analogous aqueous solution reactions result in formation of the bidentate anion exclusively, it is clear that the presence of water either lowers the intrinsic barrier or alters the reaction mechanism.

The coordination geometry about the central atom also appears to influence strongly the relative height of the barrier to bidentate anion formation. Neutral boron trifluoride, BF_3, goes from a three-coordinate trigonal planar geometry to a four-coordinate tetrahedral geometry in both the monodentate and bidentate product anions. Silicon tetrafluoride, SiF_4, is tetrahedral and upon addition of the ligand anion to the coordination sphere becomes a trigonal bipyramidal anion. Our results indicate that formation of the cyclic bidentate species occurs more readily with SiF_4 than with BF_3. A comparison of the amount of monodentate product versus the amount of bidentate product formed in the reactions of $HCat^-$ and of $MeHCat^-$ with each of the Lewis acids can be made by the examination of Figure 2. At a given pressure, the bidentate product is formed in greater abundance when SiF_4 is the Lewis acid. Of course, differences in reactivity can also be due to a change in the identity of the central atom (that is Si as opposed to B), but both solution studies[4–8] and our gas-phase studies[9,14,15] of both bimolecular and termolecular reactions involving SiF_4 and BX_3 (X = F, Cl, Br) show that the two exhibit similar chemistries. Our *ab initio* calculations for model BF_3/diolate anion and SiF_4/diolate anion complexes do not indicate any major differences in energetics for the two Lewis acid/ligand systems.[15]

---

[14] Ruhr, P. S. Bimolecular Reactions at Coordinatively Unsaturated Centers, Masters Thesis, Louisiana State University, 1986.

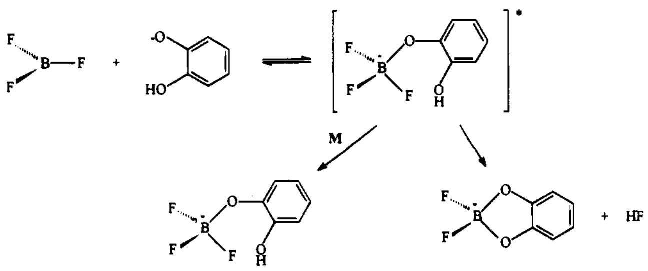

Figure 3. The concerted mechanism is illustrated here for the reaction of BF_3 with $HCat^-$.

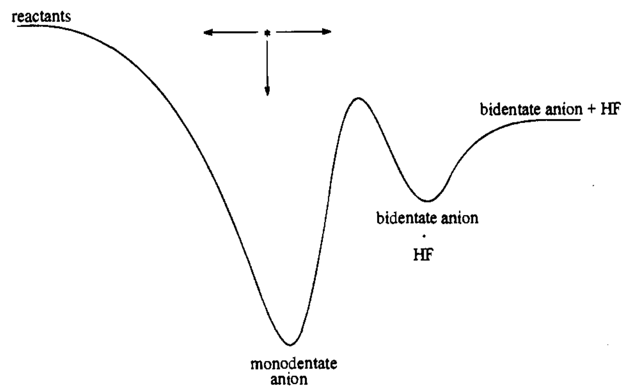

Figure 4. A generalized potential energy curve for the double-well mechanism given in Figure 3 is presented. Well depths are approximate, based upon relative values from *ab initio* calculations on model BF_3 and SiF_4 systems.[15]

Two mechanisms are consistent with our results. First is a concerted mechanism in which the second oxygen donor atom is partially bonded to the central atom (either B or Si) and the bond to the leaving F^- is partially broken. The H−F bond may be formed to some extent as well. This mechanism, shown for the reaction of BF_3 and $HCat^-$ in Figure 3, is best represented by a double-well potential energy curve as shown in Figure 4. The first well represents the monodentate species and the second represents the stable associated bimolecular products, that is, the bidentate product with HF bound by electrostatic ion−dipole forces. Initially, the two reactants combine to form the excited intermediate species designated with an asterisk. From here, three reaction paths are possible, and are thus in competition: decomposition back to reactants, ring-closure, and three-body stabilization. This double-well potential energy surface is similar to the surfaces which have been shown both experimentally[16,17] and theoretically[18−20] to govern gas-phase bimolecular nucleophilic substitution reactions at carbon;[21,22] the first and second wells represent the electrostatically associated reactants and the electrostatically associated products, respectively. These potential minima are typically on the order of 10 kcal mol^{-1} deep. The top of the barrier is the transition state with the familiar five-coordinate S_N2 carbon complex in which the incoming nucleophile and the leaving group are involved in some degree of bond formation and breakage, respectively. Because the species corresponding to potential minima along the reaction path are bound only electrostatically, they are not isolated; the presence of a central barrier is inferred on the basis of rate coefficients much smaller than those predicted by Langevin or ADO theory. Similar potential energy surfaces have been invoked to describe the behavior of other systems.[23−29]

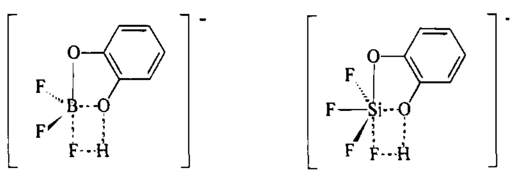

Figure 5. The two structures illustrate the 5-coordinate boron and 6-coordinate silicon transition states for the concerted mechanism for reactions with $HCat^-$.

The double-well potential energy surface describing the reactions examined here differs from that for the S_N2 process in that the first well contains a species resulting from the formation of a strong chemical bond. This results in a deeper well than one resulting from ion−dipole or ion−induced dipole interactions alone. The second well corresponds to the electrostatically bound products of elimination: the bidentate anion and HF. The barrier on this surface is the transition state to bimolecular products, just as it is in the previously described carbon systems. However, because the adduct ion is chemically bound, it can be detected, and ratios of addition to bimolecular product ions can be obtained. These ratios also reveal information about the intrinsic barrier, information which must be obtained from rate coefficient measurements alone in the carbon systems. The transition state complex is analogous to the 5-coordinate carbon transition state complexes characteristic of S_N2 reactions at carbon centers. For our BF_3 and SiF_4 reactions, transition states of this nature would require boron to adopt a 5-coordinate geometry (similar to the isoelectronic neutral carbon systems) and silicon to adopt a 6-coordinate geometry. Figure 5 shows qualitative examples of such possible transition state complexes for reactions of BF_3 and SiF_4 with $HCat^-$. Hypervalent silicon and boron complexes have been examined both theoretically and experimentally.[8,30−36] Four-coordinate boron and five-coordinate silicon anions are well precedented. The hypervalent five-coordinate B and six-coordinate Si species are currently the subject of much interest.[8,36]

The second mechanism which is consistent with our results is not a concerted mechanism, but rather it occurs in a sequence of steps; the reaction path for this mechanism is a multiple-well potential. This mechanism involves formation of the excited adduct followed by breakage of a B−F or an Si−F bond

---

(15) Taylor, W. S. Ion−Molecule Reactions of Ligating Anions with Selected Lewis Acids As Potential Energy Surface Probes, Ph.D. Dissertation, Louisiana State University, 1988.

(16) Olmstead, W. N.; Brauman, J. I. *J. Am. Chem. Soc.* **1977**, *99*, 4219.

(17) Brauman, J. I. In *Kinetics of Ion−Molecule Reactions*; Ausloos, P., Ed.; Plenum Press: New York, 1979.

(18) Evanseck, J. D.; Blake, J. F.; Jorgensen, W. L. *J. Am. Chem. Soc.* **1987**, *109*, 2349.

(19) Pellerite, M. J.; Brauman, J. I. *J. Am. Chem. Soc.* **1980**, *102*, 5993.

(20) Chandrasekhar, J.; Smith, S. F.; Jorgensen, W. L. *J. Am. Chem. Soc.* **1984**, *106*, 3049.

(21) Fehsenfeld, F. C.; Lindinger, W.; Schiff, H. I.; Hemsworth, R. S.; Bohme, D. K. *J. Chem. Phys.* **1976**, *64*, 4887.

(22) Po, P. L.; Porter, R. F. *J. Am. Chem. Soc.* **1977**, *99*, 4922.

(23) Creasy, W. R.; Farrar, J. M. *J. Chem. Phys.* **1987**, *87*, 5280.

(24) Asubiojo, O. I.; Brauman, J. I. *J. Am. Chem. Soc.* **1979**, *101*, 3715.

(25) Bass, L. M.; Cates, R. D.; Jarrold, M. F.; Kirchner, N. J.; Bowers, M. T. *J. Am. Chem. Soc.* **1983**, *105*, 7024.

(26) Herbst, E. *J. Chem. Phys.* **1985**, *82*, 4017.

(27) Smith, D.; Adams, N. G. *Astrophys. J. Lett.* **1978**, *220*, L87.

(28) Smith, D.; Adams, N. G. *Astrophys. J.* **1977**, *217*, 741.

(29) Saxer, A.; Richter, R.; Villinger, H.; Futrell, J. H.; Lindinger, W. *J. Chem. Phys.* **1987**, *87*, 2105.

(30) Sullivan, S. A.; DePuy, C. H.; Damrauer, R. *J. Am. Chem. Soc.* **1981**, *103*, 480.

(31) Damrauer, R.; DePuy, C. H.; Bierbaum, V. M. *Organometallics* **1981**, *1*, 1553.

(32) Dewar, M. J. S.; Healy, E. *Organometallics* **1982**, *1*, 705.

(33) Davis, L. P.; Burggraf, L. W.; Gordon, M. S.; Baldridge, K. K. *J. Am. Chem. Soc.* **1985**, *107*, 4415.

(34) Damrauer, R.; Burggraf, L. W.; Davis, L. P.; Gordon, M. S. *J. Am. Chem. Soc.* **1988**, *110*, 6601.

(35) Gordon, M. S.; Davis, L. P.; Burggraf, L. W.; Damrauer, R. *J. Am. Chem. Soc.* **1986**, *108*, 7889.

(36) For a recent review, see: Gordon, M. S.; Davis, L. P.; Burgraff, L. W. In *Advances in Gas Phase Ion Chemistry*; Adams, N., Babcock, L. M., Eds.; JAI Press: Greenwich, CT, 1992; and references therein.

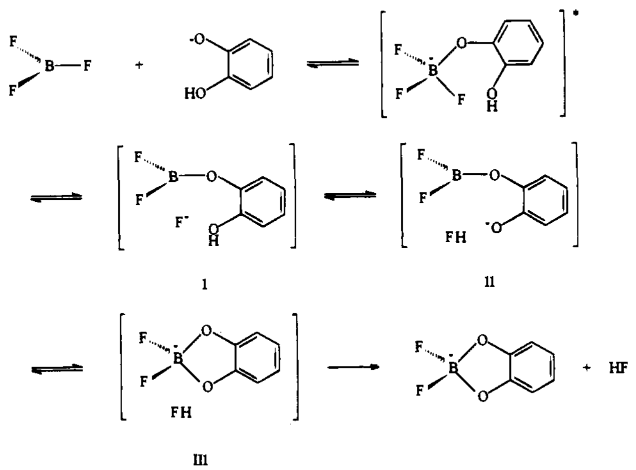

Figure 6. The sequence of mechanistic steps for the multiple-well mechanism is given; production of the mondentate product is via stabilization of the initial excited adduct (designated with an asterisk).

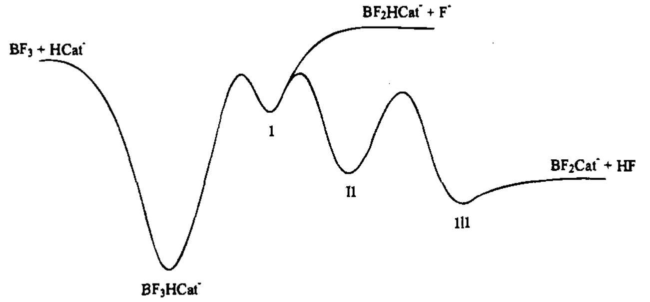

Figure 7. A representative potential energy curve for the reaction of BF_3 with $HCat^-$ occurring by the mechanism presented in Figure 6 is shown. Well depths are approximate, based upon relative values from *ab initio* calculations on model BF_3 and SiF_4 systems.[15]

to produce F^-. Energy available in the excited adduct is sufficient to break the bond between the central atom and the fluoride ion, but there is not sufficient energy remaining for F^- to escape the ion−dipole attractive forces. As a result, a cluster ion is formed. This ion−neutral cluster can then undergo further reaction. The F^- anion abstracts a proton from the remaining −OH group on the ligand and O^- bonds to the central atom in a ring-closure step. Energy released in the formation of the HF bond and in chelation is sufficient for the neutral HF and the bidentate product anion to separate. This mechanism is illustrated in Figure 6 for the reaction of BF_3 with $HCat^-$ to form the bidentate product anion; the monodentate anion results from stabilization of the excited adduct (designated with an asterisk) initially formed. A potential energy curve corresponding to this mechanism is shown in Figure 7. Calculations using heats of formation and estimated heats of formation for the neutral and anionic complexes in the reaction mechanism indicate that energetics for both the BF_3 and SiF_4 systems are consistent with this mechanism.[37] That is, formation of the borate or silicate anion by addition of the ligand anion to the Lewis acid is exothermic, while addition of the ligand anion and elimination of an F^- anion is close to thermoneutral. The complex, once formed, has enough energy to break the $B-F^-$ or $Si-F^-$ bond but is then trapped in the shallow ion−dipole well indicated in Figure 7. Abstraction of a proton and formation of the HF bond is energetically favorable, and subsequent ring closure corresponding to passage over a barrier into the bidentate anion product well is possible. The qualitative energy features of the curve in Figure 7 describe the reactions of both BF_3 and SiF_4 with bifunctional oxygen-donor ligand anions. The general idea of the deep minimum corresponding to monodentate product ion and passage over a barrier to form the bidentate product anion and HF is the same as in the double-well picture, but the transition state complex is different in that boron is 4-coordinate and silicon is 5-coordinate. Mechanisms of this type where ion−neutral clusters are formed but trapped by ion−dipole forces and undergo subsequent reactions have been successful in describing proton transfer and isotope incorporation in the case of organic ions.[38,39]

Both mechanisms can account for the relative ratios of monodentate product to bidentate product observed in our reactions and are supported by known chemistries of boron and silicon anions.[8,30−36]

Fluoride Transfers. In the reactions studied here, all of the monodentate species participate in a fluoride transfer step in which BF_4^- or SiF_5^- is formed. The neutral products in these fluoride transfers are presumed to be either boron or silicon "ethers" in which the boron is trigonal planar and the silicon is tetrahedrally coordinated. The fluoride affinities of BF_3[40,41] and SiF_4[41] are 71 and 62 kcal mol^{-1}, respectively; thus, we can set an upper limit of 62 kcal mol^{-1} on the fluoride affinities for all the silicon monodentate neutral ether species and an upper limit on the boron species of 71 kcal mol^{-1}. This indicates that BF_3 and SiF_4 are better Lewis acids with respect to F^- than the neutral ether products of the fluoride transfer reaction. This is understandable when one considers that oxygen can contribute electron density from its lone pairs of electrons to the Lewis acid center thus lowering the Lewis acidity of the central B or Si. Fluorine also has lone pairs of electrons, but is not as good a donor.

We also note that in the reactions of both BF_3 and SiF_4 with $HCat^-$ and $MeHCat^-$, fluoride transfer from the bidentate products of these reactions to either BF_3 or SiF_4 does not occur. Using the fluoride affinities of BF_3 and SiF_4 again, we can set a lower limit of 71 kcal mol^{-1} on the fluoride affinities of the bidentate neutral diethers of $HCat^-$ and $MeHCat^-$ with BF_3 and one of 62 kcal mol^{-1} for the SiF_4 systems. The possibility exists, however, that absence of reaction may be due to factors other than energetics of F^- transfer. Indeed, one expects that the energetics of ring formation in the bidentate neutral product will play a significant role as well.

Summary

We have demonstrated that the reactions of the anions of several substituted phenolic compounds with the Lewis acids BF_3 and SiF_4 can be described generally in terms of the reaction sequence shown in eq 6. Formation of a monodentate three-body product is followed by further reaction of this anion with the reactant neutral in a fluoride transfer step. While a bimolecular product channel is not available to the $HRes^-$ and $HCres^-$ systems, the reactions of $HCat^-$ and $MeHCat^-$ with both Lewis acids result in the formation of a fully chelated bidentate anionic species. Both the monodentate and bidentate products from the reaction of $HCat^-$ with BF_3 were observed to form clusters with BF_3 in nitrogen carrier gas. In the reactions of $HCat^-$ and $MeHCat^-$ with both BF_3 and SiF_4, a competition between the two product channels exists over the range of pressures examined here. The relative amounts of these two products is a function of pressure. This can be explained by a multiple-well potential energy curve containing a barrier in the

---

(37) JANAF Thermochemical Tables. *Natl. Stand. Ref. Data Ser.* **1971**, *37*; JANAF Thermochemical Tables. *J. Phys. Ref. Data* **1974**, *3*.

(38) Henchman, M.; Smith, D.; Adams, N. G. *Int. J. Mass Spectrom. Ion Processes* **1991**, *109*, 105.

(39) Henchman, M.; Smith, D.; Adams, N. G.; Paulson, J. F.; Lindinger, W. In *Rate Coefficients in Astrochemistry*; Millar, T. J., Williams, D. A., Eds.; Kluwer Academic Publishers: Boston, 1988.

(40) Haartz, J. C.; McDaniel, D. H. *J. Am. Chem. Soc.* **1973**, *95*, 8562.

(41) Larson, J. W.; McMahon, T. B. *J. Am. Chem. Soc.* **1985**, *107*, 766.

ring-closure exit channel. Two mechanisms consistent with our results are presented. The height of the barrier in the bimolecular product channel dictates the relative amounts of each product formed, and thus the product ratios are an excellent means by which to probe factors affecting barrier height and thus the nature of the transition state complex. If the trends in product distributions with respect to pressure noted here hold true for a wide range of pressures, one expects that in the limit of low pressure only bidentate anion product would form at some fraction of the collision rate (that fraction would be dependent upon the barrier height). In the limit of high pressure, only monodentate anion product should be produced, with the reaction proceeding at the bimolecular collision rate.

Acknowledgment is made to the donors of the Petroleum Research Fund, administered by the American Chemical Society, for partial support of this research. We also acknowledge very helpful discussions with Dr. J. M. Manion of the University of Central Arkansas.

JA9319912